ELSEVIER

Earth and Planetary Science Letters 154 (1998) 237–246

EPSL

Annual trace element variations in a Holocene speleothem

Mark S. Roberts [a,*], Peter L. Smart [b,1], Andy Baker [c,2]

[a] Department of Geography, University of Bristol, University Road, Bristol BS8 1SS, UK
[b] Department of Geography, University of Bristol, University Road, Bristol BS8 1SS, UK
[c] Department of Geography, University of Exeter, Amory Building, Rennes Drive, Exeter EX4 4RJ, UK

Received 2 February 1997; accepted 20 June 1997

Abstract

High resolution secondary ionization mass spectrometry (SIMS) analysis along the growth axis of a Holocene speleothem from northern Scotland reveals high frequency oscillations and longer term trends in Mg/Ca, Sr/Ca and Ba/Ca. At the scale of the high frequency oscillations, Mg/Ca and Sr/Ca display a well-defined anticorrelation, while Sr/Ca and Ba/Ca are positively correlated. Imaging of elemental ratios in two dimensions reveals that the high frequency signal is well preserved and laterally continuous across the sample. TIMS ^{230}Th ages and annual ultraviolet luminescence banding provide chronological control and demonstrate that the high frequency cyclicity is annual. Trace element variations in speleothem calcite are a reflection of hydrochemical processes in the unsaturated zone overlying the cave (supply effects) and partitioning at the water–calcite interface. Mg partitioning between water and calcite is temperature dependent. Calculations suggest that the annual Mg/Ca oscillations may be caused by seasonal temperature changes. However, the longer timescale variations in Mg/Ca are too great to be explained by this mechanism. Seasonal variations in water residence time in the unsaturated zone (which reflect effective precipitation) provide a more probable explanation for the observed annual oscillations and also explain the inverse relationship between Mg/Ca and Sr/Ca. This record suggests that trace elements in speleothems have the potential to provide the high resolution insights into interannual palaeoclimatic variability required for assessment of general circulation models. © 1998 Elsevier Science B.V.

Keywords: secondary ion mass spectroscopy; speleothems; palaeoclimatology; luminescence

1. Introduction

In order to improve our understanding of the operation of the global climate system, high resolution terrestrial records are needed to complement data originating from ocean cores. The advent of TIMS ^{230}Th–^{234}U dating [1], and the challenge to Milankovitch theory mounted by the Devil's Hole δ^{18}O record [2] has served to refocus attention on the potential of speleothems (secondary cave deposits e.g. stalagmites and flowstones) to provide a high resolution archive of terrestrial palaeoclimate information. This potential has been further augmented by the recent recognition [3] of ultraviolet luminescence banding in speleothems, which may give annual chronological control. Past research has tended to focus on studies of the oxygen isotope composition of speleothems e.g. [4–7] in attempts to derive palaeotemperature records. In contrast, the

* Corresponding author. Fax: +44 117 928 7878. E-mail: m.s.roberts@bristol.ac.uk
[1] Fax: +44 117 928 7878. E-mail: p.l.smart@bristol.ac.uk
[2] Fax: +44 1392 263342. E-mail: a.baker@ex.ac.uk

PII S0012-821X(97)00116-7

potential of the trace element content of speleothems is largely unexplored [8] (although see [9–11]). Annual trace element cyclicity has been observed in corals [12–15] and is believed to reflect seasonal variations in environmental parameters such as sea surface temperature. In this study, we use secondary ionisation mass spectrometry (SIMS) to demonstrate that an annual signal in trace element geochemistry (Mg/Ca, Sr/Ca and Ba/Ca) is preserved within a speleothem from a shallow cave in north-west Scotland. We outline the factors that may produce this signal and suggest their potential palaeoclimatic significance.

2. Sample description

SU-80-11 is a small stalagmite (168 mm high) collected from Uamh an Tartair cave (58°9′ N 4°55′ W) which is situated in the Traligill basin near Inchnadamph, north-west Scotland (see Fig. 1). The cave has developed within the partially dolomitised Eilean Dubh Formation of the Cambro-Ordovician Durness Group. The sample consists of dense, cream coloured calcite with elongate crystals arranged in a "palisade" structure which is characteristic of many speleothems [16]. There is no evidence of any depositional hiatuses and growth is assumed to be continuous along the length of the sample.

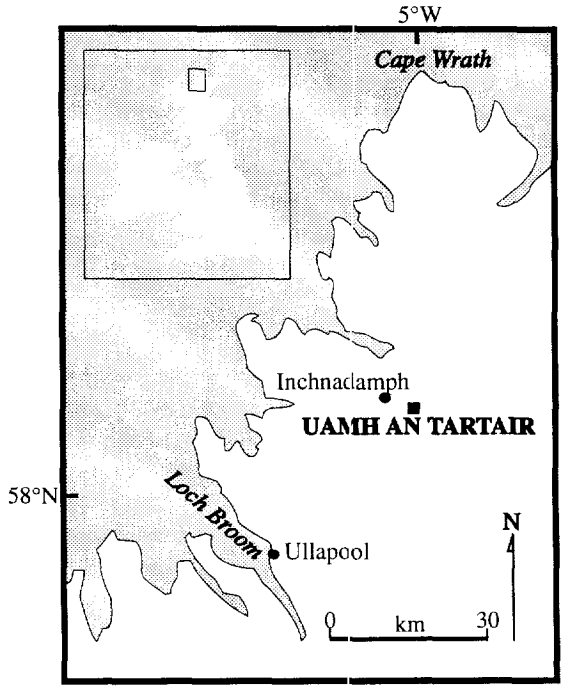

Fig. 1. Map showing the location of Uamh an Tartair.

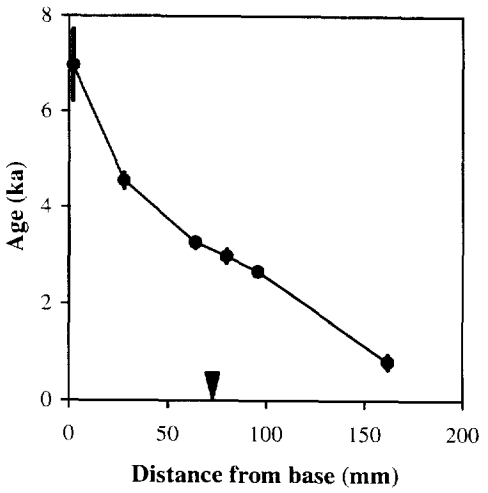

Fig. 2. Distance/age model for SU-80-11 based on 7 TIMS ^{230}Th ages [3,17]. The arrow indicates the location of the section analysed. The age at 80 mm is the mean of two replicates. Error bars are 2σ.

TIMS ^{230}Th^{234}U dating has revealed that the sample grew at a non-linear rate through the course of the Holocene (Fig. 2) [3,17]. The section under consideration in this study is bracketed by TIMS ^{230}Th ages of 3.27 ± 0.11 ka (errors are 2σ) at 64 mm (SU-80-11C) and 2.99 ± 0.15 ka at 80 mm (mean of two replicates (SU-80-11D (1) and (2)). These ages suggest a mean extension rate of 57 ± 19 μm a^{-1} (1σ) between these dated points (assuming a linear extension rate), the maximum rate observed in the sample. The analysed section also displays clear annual luminescence banding which indicates a mean extension rate of 55 ± 3 μm a^{-1} (2 standard errors; $n = 242$) [3] in good agreement with the less precise estimate derived from the TIMS ^{230}Th ages. This particular part of SU-80-11 was selected for further analysis as the extension rate permitted sub-annual resolution to be achieved using SIMS and also comparison to be made between the trace element and ultraviolet luminescence records.

3. Analytical methods

SIMS provided the combination of high precision in situ analysis and high spatial resolution required to achieve subannual resolution in this section of SU-80-11. Prior to analysis, the section of SU-80-11 was cut, mounted in epoxy resin (Petropoxy 154®), polished and gold coated. All analyses were performed on a Cameca ims-4f ion microprobe at the University of Edinburgh.

A 15 keV O^- primary beam was produced by a duoplasmatron source with positive secondary ions being counted on an electron multiplier. The primary beam current was maintained at 30–35 nA throughout the course of the analyses and sputtered an area of 30–40 μm on the surface of the sample. Spatial resolution is controlled by the diameter of a (field) aperture placed in the secondary column and was nominally 1 μm. In practice, because the secondary beam includes some ions of high angular velocity, the actual spatial resolution was somewhat lower (2–4 μm). The comparatively large primary beam diameter relative to the actual spatial resolution meant that each analysis point was sputtered for >5 min prior to analysis ensuring complete removal of the gold coating. At each analysis point ^{26}Mg, ^{44}Ca, ^{88}Sr and ^{138}Ba were analysed with counting times of 2s, 1s, 1s and 3s respectively. Typical count rates were 6×10^3 (^{26}Mg), 1×10^5 (^{44}Ca), 3×10^4 (^{88}Sr) and 5×10^3 (^{138}Ba) cps. At these high count rates and with a stable primary beam current, the precision of individual analyses is considered to be limited only by counting statistics [18], therefore 1×10^4 total counts will produce a theoretical analytical error of 1%. Veizer et al. [19] and Swart [20] listed the possible interferences for SIMS Mg, Ca and Sr analyses in carbonate minerals. However, the trace element concentrations present even in the lowest concentration areas of the sample were sufficiently high that such interferences constituted $<0.5\%$ of the total ion signal. Therefore, in contrast to many SIMS analyses made at low mass resolution, no energy offset was used. Each isotope was measured twice at each point, corrected for isotopic abundance and standardized against a calcite standard (a calcite from the Oka Carbonatite Complex in the Monteregian Hills, Quebec, Canada (Mg = 618 μg g^{-1}, Sr = 10 300 μg g^{-1}, Ba = 1014 μg g^{-1})).

A total of 1200 points, 2 μm apart, were analysed parallel to the growth axis of the sample, producing a track of 2400 μm in length. Sample movement was controlled by a computer driven stepper motor. The track was located to avoid any surface irregularities. Given the actual spatial resolution of 2–4 μm, the 2 μm step size resulted in overlapping of successive points and therefore, a certain degree of spatial averaging.

Ultraviolet luminescence images of the SIMS analysis track were obtained using a Zeiss Axiotech® microscope with a Hg ultraviolet light source and a 410 nm filter. The field of view was $\sim$ 500 μm. Six overlapping images were combined into a mosaic spanning the entire length of the analysis track.

4. Results

The new ultraviolet luminescence photomosaic spanning the SIMS analysis track showed 41 ± 3 distinct annual bands (the error is derived from the range of values observed by five different observers). On the basis of the luminescence banding, Baker et al. [3] suggested that the mean extension rate in this section of the sample was 55 ± 3 μm a^{-1}, the analysis track thus represents 44 ± 3 years. Both these estimates are in excellent agreement with TIMS derived estimate of 42 ± 27 years.

The results of the SIMS analyses are plotted against distance along the 2400 μm analysis track with the fine line in the lefthand panels of Fig. 3 and summary descriptive statistics for the three datasets are reported in Table 1. The results show that Mg/Ca, Sr/Ca and Ba/Ca ratios display considerable structure at a high frequency. There are also longer timescale trends within the data (for example, the general trend towards higher Mg/Ca values in the second half of the analysis track (Fig. 3A)). In order to enhance the high frequency structure, the longer timescale trends were removed by filtering the data with a fifty point running mean (illustrated by the heavy line in the lefthand panels of Fig. 3). The results of this detrending procedure are illustrated in the righthand panels of Fig. 3. In addition to the strong high frequency cyclicity, the detrended data also reveals regular variations in the amplitude of the high frequency oscillations along the length of

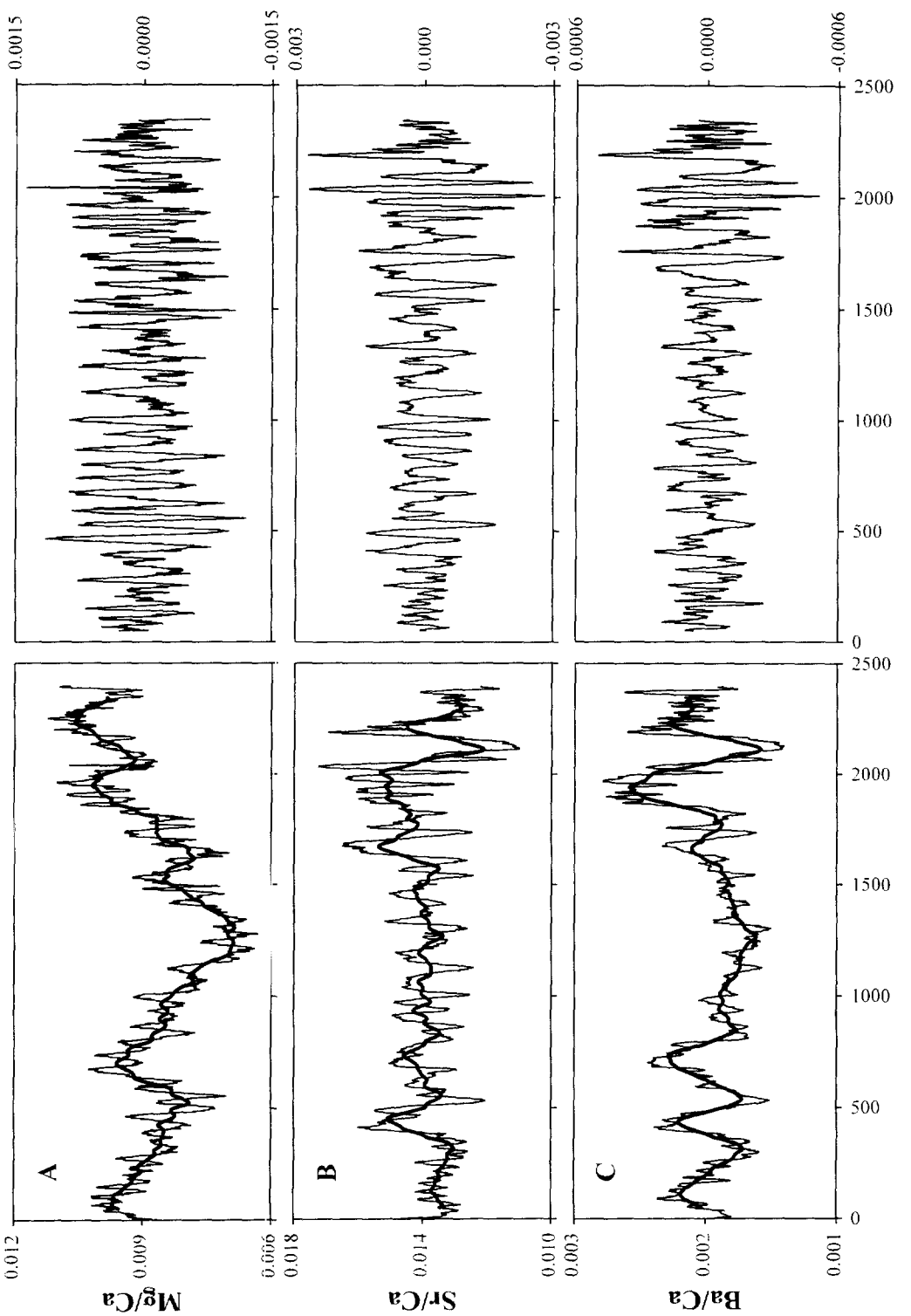

Fig. 3. Changes in (A) Mg/Ca, (B) Sr/Ca and (C) Ba/Ca (*weight % ratios*) with distance along the SIMS analysis track. The start of the track represents the oldest sample. The *fine line the lefthand panels* represents the original data and the thick line is the fifty point running mean of data. The right hand panels illustrate the detrended SIMS data.

Table 1
Descriptive statistics for SU-80-11 SIMS dataset ($n = 1200$)

	Mean	S.D. (1σ)	Maximum	Minimum
Mg/Ca	0.0088	0.0010	0.011	0.0063
Sr/Ca	0.014	0.0011	0.017	0.011
Ba/Ca	0.0020	0.00028	0.0028	0.0014

All SIMS data are expressed as weight % ratios.

Table 2
Correlation coefficients (r) for the low frequency record (heavy line in the lefthand panels of Fig. 3) and the detrended high frequency record (see righthand panels in Fig. 3) ($n = 1150$)

	Low frequency	High frequency
Mg/Ca:Sr/Ca	−0.013	−0.47
Mg/Ca:Ba/Ca	0.70	0.82
Sr/Ca:Ba/Ca	0.59	−0.12

the analysis track. The maximum amplitude oscillations occur at around 500 μm and 2000 μm with a minimum occurring at 1200 μm.

Longer timescale trends in the SIMS data can be illustrated by examining the behaviour of the fifty point running means that were used to detrend the original data (the heavy line in the lefthand panels in Fig. 3). This data shows that in addition to the high frequency structure in the data there are longer wavelength features. The Mg/Ca record shows distinct peaks at 700 μm, 1500 μm, 1920 μm and 2230 μm. The Sr/Ca and Ba/Ca records show similar patterns with additional peaks at 430 μm, and 1630 μm (possibly matching a shoulder in the Mg/Ca record), however the peak at 1500 μm is absent. Both the Mg/Ca and Ba/Ca data show a trend towards higher values in the second half of the records while the Sr/Ca record has no long term trend.

For the long term trends, Mg/Ca and Ba/Ca and Sr/Ca and Ba/Ca are positively correlated (see Table 2) while Mg/Ca and Sr/Ca are uncorrelated. In contrast, in the detrended dataset there is a significant inverse relationship between Mg/Ca and Sr/Ca at the scale of the high frequency oscillations while Sr/Ca and Ba/Ca are positively correlated. Mg/Ca and Ba/Ca display a weak inverse relationship. We note that the different interrelationships observed at low and high frequencies (Table 2) suggest that distinct processes may control the geochemistry of speleothem calcite on different timescales. The inverse relationship between Mg/Ca and Sr/Ca observed at high frequencies is illustrated in Fig. 4 which also shows the resolution of the analysis points relative to the wavelength of the high frequency oscillations. These interrelationships display a size (ionic radius) dependent pattern. Sr^{2+} and Ba^{2+} (larger than Ca^{2+}) correlate with each other and anticorrelate with Mg^{2+} (smaller than Ca^{2+}).

The lateral integrity of the short wavelength oscillations was assessed by imaging Mg/Ca, Sr/Ca and

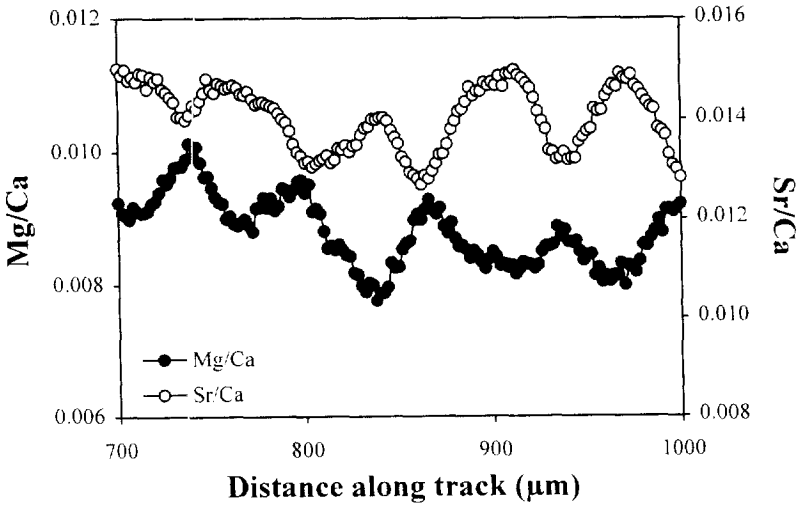

Fig. 4. Comparison of the Mg/Ca and Sr/Ca records between 700 and 1000 μm, clearly showing the existence of the inverse relationship between these two variables.

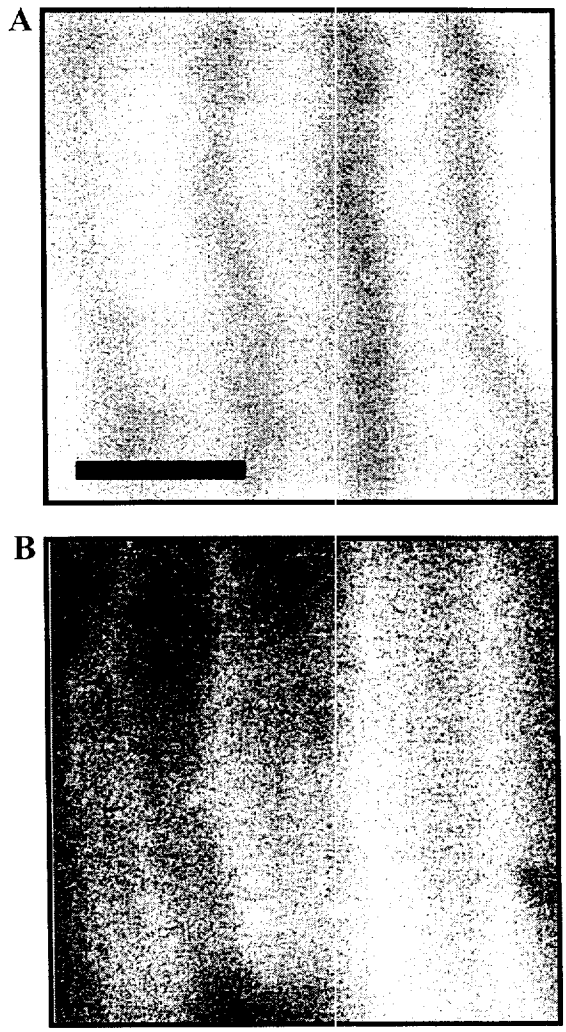

Fig. 5. (A) SIMS image of Sr/Ca centred on 900 μm along the analysis track (the lighther areas correspond to higher ratio values (the maximum Sr/Ca value in this area is 0.015)). Scale bar is 50 μm. the image was captured with the dynamic transfer system of the ion probe on to accomodate changes in the position of the ion source as beam was rastered across the sample surface. (B) Ultraviolet photomicrograph of the same area as illustrated in (A). Light bands are high luminescence (interpreted as representing high humic and fulvic acid content).

Ba/Ca in two dimensions by rastering the beam over a small area of the sample. This procedure demonstrated that the short wavelength oscillations are laterally contiguous and comparable in magnitude across the sample, and are not an artefact of the particular track analysed (the Sr/Ca image is presented in Fig. 5A). In order to assess the relationship between ultraviolet luminescence (considered here to be purely a proxy for the humic and fulvic acid content of the calcite [3]) and the SIMS trace element records, an ultraviolet photomicrograph of the area that was imaged by SIMS (see Fig. 5B) was obtained. This photomicrograph indicates that the low intensity luminescence bands correspond to high Sr/Ca (and therefore low Mg/Ca areas).

At selected locations on the sample ^{30}Si was also analysed to determine if the high frequency oscillations might result from variations in the detrital (non-carbonate) content of the calcite (e.g. clay particles), although the TIMS ^{230}Th/^{232}Th activity ratios suggested that this was negligible [3]. Only occasional counts were collected at mass 30, and at the majority of locations, no ^{30}Si was detected, thus confirming the low detrital content. This suggests that the observed Mg/Ca, Sr/Ca and Ba/Ca variations reflect genuine spatial differences in the trace element composition of the calcite lattice.

4.1. The nature of the high frequency trace element oscillations

As noted above, the ultraviolet luminescence banding constrained the timespan represented by SIMS analysis track to 43 ± 4 years (mean of the two estimates). For comparison, the number of visually distinct peaks in the detrended trace element records (see Fig. 3) were also counted. The Mg/Ca record showed 42 ± 3 peaks, the Sr/Ca record showed 45 ± 4 peaks and the Ba/Ca record 45 ± 6 peaks (errors are based on variations between five different observers). The detrended record is only 2300 μm long (due to the use of the fifty point running mean), therefore it is useful to extrapolate the data to the predicted number of peaks for the whole 2400 μm track ((number of peaks counted /2300) $\times$ 2400). This extrapolation merely adds two to the number of peaks for the whole 2400 μm track for each ratio with no change in the error (i.e. Mg/Ca = 44 ± 3, Sr/Ca = 45 ± 4 and Ba/Ca = 47 ± 6). Therefore the number of peaks observed at high frequencies in the detrended SIMS records corresponds to the overall timespan represented by the track, suggesting that the high frequency trace element oscillations observed in this section of SU-80-11 are annual in nature. This is confirmed by determination of the dominant frequency in the detrended data

using spectral analysis. In the Mg/Ca, Sr/Ca and Ba/Ca data, a single significant peak in spectral density was observed at frequencies of 0.0176, 0.0169 and 0.0161 respectively (these frequencies were consistent and significant at a range of bandwidths). These frequencies correspond to distance intervals of 57, 59 and 62 μm in excellent agreement with the extension rate determined on the basis of the annual luminescence bands of 56 ± 6 μm a^{-1}. On the basis of these results we conclude that the high frequency trace element oscillations observed in SU-80-11 are annual.

5. Discussion

Annual trace element cyclicity has been observed in corals (e.g. [12–15]) and has been interpreted as reflecting changes in sea surface temperature and other environmental parameters. The following discussion focuses on the possible hydrochemical processes that may produce the annual trace element variations observed in SU-80-11.

5.1. Effect of seasonal temperature variations

Partitioning of Mg between water and calcite is temperature dependent [21] and previous attempts to examine trace element variations in speleothems have focused on this observation [9–11]. A number of experimental studies have attempted to quantify this temperature dependence [22–24]. In addition, Gascoyne [9] employed analysis of cave waters and actively forming speleothem calcite in two different climatic regimes to determine the temperature dependency of D_{Mg} (the homogenous partition coefficient [25]). The original site of SU-80-11 is within 50 m of the cave entrance [26]. Therefore, unlike deep cave environments where temperatures are constant throughout the year, seasonal temperature variations may have been experienced by the sample (depending on the degree of cave ventilation [27]) and thus affected D_{Mg}. The mean observed amplitude of the annual Mg/Ca oscillations in this section of SU-80-11 was 0.00135 ± 0.00045 (1σ). Using linear regression equations fitted to the data in [9,22–24] and representative water composition data from bedrock seeps in the Traligill basin [28] (Mg/Ca_{water} (molar ratio) ranging between a minimum of 0.75 and a maximum of 1), we calculate the annual temperature range required to produce an annual Mg/Ca oscillation of 0.00135 ± 0.00045 (see Table 3) for a mean annual temperature of 8.6°C. There is considerable variation in the predicted ranges (although the data based on [23,24] are in good agreement) but all are less than the mean annual surface temperature range in north-west Scotland (4.5–13.5°C). The latter represents the maximum temperature range which could affect the sample, therefore we cannot exclude the possibility that the annual Mg/Ca variations in SU-80-11 may be produced by seasonal temperature changes.

Temperature cannot be directly invoked as a factor to explain observed annual Sr/Ca and Ba/Ca variability, as Sr and Ba partitioning into calcite are independent of temperature [21,30]. However, an indirect thermal effect may exist through the impact of temperature variations on the calcite precipitation rate which experimental studies [31,32] have demonstrated to affect D_{Sr} and D_{Ba}. The rate of speleothem calcite precipitation is a complex function of temperature, recharge rate, PCO_2 and Ca^{2+} concentration [33]. Both PCO_2 and Ca^{2+} concentration are sensitive to temperature variations such that the rate of speleothem calcite deposition increases with temperature. Therefore on a simple basis, as Mg/Ca increases (due to the temperature control on D_{Mg}), so should Sr/Ca and Ba/Ca, as precipitation rate increases. However, in SU-80-11, we observe an inverse relationship between Mg/Ca and the other two ratios.

Furthermore, temperature changes cannot be invoked to explain the longer term trends within the Mg/Ca record. The mean Mg/Ca ratio between 1200 and 1300 μm is 0.0069 ± 0.00037 (1σ) compared to 0.0096 ± 0.00049 (1σ) in the final 100 μm (2300–2400 μm) of the record. If temperature alone was controlling Mg/Ca, mean annual temperatures would have had to have increased dramatically over a period of 20 years between 3.0 and 3.2 ka (see results in Table 4). Such temperature changes are not recorded during the course of the Holocene in the British Isles (the maximum temperature increase is believed to be associated with the mid-Holocene climatic optimum (8–4.5 ka) which was 2°C warmer than present [34]). Thus, the role of temperature in controlling speleothem trace element variations is

Table 3
Annual temperature range required to produce mean observed Mg/Ca variations

	Reference							
	[9]		[22]		[23]		[24]	
Linear regression equation[a]	$D_{Mg} = 0.0017T +$ 0.0052		$D_{Mg} = 0.0007T +$ 0.0033		$D_{Mg} = 0.00042T +$ 0.009		$D_{Mg} = 0.00043T +$ 0.0011	
Molar Mg/Ca_{water}[b]	0.75	1	0.75	1	0.75	1	0.75	1
Required temperature range (°c)[c]	1.8	1.2	4.0	3.2	7.0	5.4	6.8	5.2
Predicted $Mg/Ca_{calcite}$[d]	**0.0084**	0.0115	0.0036	0.005	0.0051	**0.007**	0.0058	**0.008**
Predicted $Mg/Ca_{calcite}$[e]	**0.0098**	0.0127	0.0049	**0.0064**	**0.0064**	**0.0083**	**0.0078**	**0.0093**

The mean annual surface temperature range in north-west Scotland is 9°C.
[a]Linear regression equations fitted to data from [9,22–24], where T is temperature (°C) and D_{Mg} is the homogeneous partition coefficient between water and calcite and $D_{Mg} = (Mg/Ca_{calcite})/(Mg/Ca_{water})$. We assume D_{Mg} is invariant at $Mg/Ca_{water} \leq 1$ [29].
[b]Minimum Mg/Ca_{water} (= 0.75) and maximum Mg/Ca_{water} (= 1) in the Traligill basin (see Ref. [28]).
[c]Annual temperature range (°C) needed to produce an annual Mg/Ca range of 0.00135 ± 0.00049. (Values were calculated iteratively forcing the mean to equal 8.6°C (mean annual temperature).)
[d]Predicted $Mg/Ca_{calcite}$ at the minimum required temperature (see footnote c) (values in bold fall within the range observed in the SIMS dataset.
[e]Predicted $Mg/Ca_{calcite}$ at the maximum required temperature (see footnote c) (values in bold fall within the range observed in the SIMS dataset.

not proven. The annual Mg/Ca variations may be produced by seasonal temperature changes but the longer term trends in Mg/Ca are too great to be explained by simple temperature dependent Mg partitioning (although note the possibility of different processes operating on different timescales).

5.2. Supply effects and groundwater residence time

It is important to note that trace element partitioning at the water–calcite interface cannot be investigated in isolation from the remainder of the hydrochemical system. The processes which ultimately control the **supply** of trace elements to that interface must also be addressed. Railsback et al. [35] suggested that annual mineralogical and trace element (Mg and Sr) changes in a Botswanan Holocene stalagmite were driven by evaporative concentration of dripwaters. Studies in Soreq Cave, Israel also indicate the importance of evaporative concentration in controlling the Mg content of dripwaters (M. Bar-Matthews, personal communication). However, both these sites are in semi-arid locations and it seems unlikely that this explanation would be tenable in the humid-temperate setting of north-west Scotland where temperatures are low and precipitation is high (> 1500 mm) and occurs in all seasons.

Table 4
Temperature change (°C) required to drive $Mg/Ca_{calcite}$ from 0.0069 to 0.0096

Mg/Ca_{water}[a]	Reference			
	[9]	[22]	[23]	[24]
0.75	3.9	16.5	9.4	15.3
1	2.9	12.4	7.1	11.5

[a]Representative water composition (molar) for the Traligill basin from Ref. [28].

The classic study of Plummer [36] demonstrated that the Mg/Ca ratio of groundwaters in the Floridan aquifer increased with residence time. This is explained by the incongruent dissolution of dolomite in the presence of calcite [37]. Initially both calcite and dolomite dissolve congruently. After saturation with respect to calcite is attained, continued dissolution of dolomite increases the Mg concentration in solution, while Ca is held constant by precipitation of calcite. The Mg/Ca_{water} ratio thus increases until dolomite saturation is reached. Residence time in the Florida aquifer is very long, but this process has also been used to explain Mg/Ca variations in karst waters with much shorter residence times [38–40]. Low Mg/Ca_{water} ratios are generally associated with short residence times in winter and following recharge, while high Mg/Ca_{water} ratios which approach those in the dolomitic bedrock are associated

with long residence times in summer. Observations during storm events at both seeps [28] and resurgences (Smart, unpublished data) in the Traligill basin study area confirm that the Mg/Ca_{water} ratio is controlled by residence time. Recent studies in dolomitic cave sites in northern Italy corroborate these findings [41]. This observed relationship may also be explained by the differential rates of calcite and dolomite dissolution. Experimental studies suggest that dolomite dissolves much more slowly than calcite [40,42,43]. Thus, during the congruent dissolution phase, the Mg/Ca_{water} ratio will initially be low but will increase as calcite saturation is approached. Dolomite generally has lower Sr and Ba concentrations than calcite [44,45]. Thus, the inverse relationship between both Mg/Ca–Sr/Ca and Mg/Ca–Ba/Ca observed on the short-term (annual) timescale in SU-80-11 (see Table 2) can be readily explained by the above arguments. Longer water residence times would be expected during the summer due to the seasonal reduction in effective precipitation associated with higher potential evaporation and reduced precipitation. Therefore, we suggest that, on an annual timescale in SU-80-11, a low Mg/Ca, high Sr/Ca signal represents short water residence time in the unsaturated zone associated with higher effective precipitation in winter, and a high Mg/Ca, low Sr/Ca signal reflects the longer residence times experienced in summer. Thus, it may be possible to reconstruct interannual variations in precipitation on the basis of the trace element content of speleothems.

6. Conclusions

This study demonstrates the potential of the trace element content of speleothems to provide high resolution terrestrial palaeochemical records comparable with the established marine records provided by corals. We have demonstrated that Mg/Ca, Sr/Ca and Ba/Ca vary on an annual timescale. Although the annual Mg/Ca variations may possibly be explained by seasonal temperature changes, we suggest that the variations reflect seasonal differences in water residence time which are controlled by changes in effective precipitation. The prospect of retrieving high resolution terrestrial palaeoclimatic information from the trace element content of speleothems merits further exploration. Calibration studies in the contemporary cave environment, laboratory experiments and assessment of signal reproducibility on annual timescales between coeval samples is the focus of current and future research.

Acknowledgements

Richard Hinton, John Craven and Jon Blundy provided critical advice and assistance before, during and after the SIMS analyses. Amanda Dennis helped with the spectral analyses. We are grateful to two anonymous referees for their comments. We also thank NERC for instrument time and a studentship (GT4/93/114/P) to MSR. AB also thanks the Royal Society for funding. *[MK]*

References

[1] R.L. Edwards, J.H. Chen, G.J. Wasserburg, ^{238}U–^{234}U–^{230}Th–^{232}Th systematics and the precise determination of time over the past 500,000 years, Earth Planet. Sci. Lett. 81 (1987) 175–192.

[2] I.J. Winograd, T.B. Coplen, J.M. Landwehr, A.C. Riggs, K.R. Ludwig, B.J. Szabo, P.T. Kolesar, K.M. Revesz, Continuous 500,000 year climate record from vein calcite in Devils Hole, Nevada, Science 258 (1992) 255–260.

[3] A. Baker, P.L. Smart, R.L. Edwards, D.A. Richards, Annual growth banding in a cave stalagmite, Nature 364 (1993) 518–520.

[4] C.H. Hendy, A.T. Wilson, Palaeoclimatic data from speleothems, Nature 219 (1968) 48–51.

[5] M. Gascoyne, H.P. Schwarcz, D.C. Ford, A paleotemperature curve for the mid-Wisconsin in Vancouver Island, Nature 285 (1980) 474–476.

[6] J.A. Dorale, L.A. Gonzalez, M.K. Regan, D.A. Pickett, M.T. Murell, R.G. Baker, A high resolution record of Holocene climate change in speleothem calcite from Coldwater Cave, north-east Iowa, Science 258 (1992) 1626–1630.

[7] A. Goede, F. McDermott, C. Hawkesworth, J. Webb, B. Finlayson, Evidence of Younger Dryas and Neoglacial cooling in a late Quaternary palaeotemperature record from a speleothem in eastern Victoria, Australia, J. Quat. Sci. 11 (1996) 1–7.

[8] M. Gascoyne, Palaeoclimate determination from cave calcite deposits, Quat. Sci. Rev. 11 (1992) 609–632.

[9] M. Gascoyne, Trace element partition coefficients in the calcite-water system and their paleoclimatic significance in cave studies, J. Hydrol. 61 (1983) 213–222.

[10] A. Goede, J.C. Vogel, Trace element variations and dating of a late Pleistocene Tasmanian speleothem, Palaeogeog. Palaeoclim. Palaeoecol. 88 (1991) 121–131.

[11] A. Goede, Continuous early last glacial palaeoenvironmental record from a Tasmanian speleothem based on stable isotope and minor element variations, Quat. Sci. Rev. 13 (1994) 283–291.

[12] J.W. Beck, R.L. Edwards, E. Ito, F.W. Taylor, J. Recy, F. Rougerie, P. Joannot, C. Henin, Sea-surface temperature from coral skeletal strontium/calcium ratios, Science 257 (1992) 644–647.

[13] T.P. Guilderson, R.G. Fairbanks, J.L. Rubenstone, Tropical temperature variations since 20,000 years ago: modulating interhemispheric climate change, Science 263 (1994) 663–665.

[14] G.T. Shen, R.B. Dunbar, Environmental controls on uranium in coral reefs, Geochim. Cosmochim. Acta 59 (1995) 2009–2024.

[15] S.R. Hart, A.L. Cohen, An ion probe study of annual cycles of Sr/Ca and other trace elements in corals, Geochim. Cosmochim. Acta 60 (1996) 3075–3084.

[16] A.C. Kendall, P.L. Broughton, Origin of fabrics in speleothems of columnar calcite crystals, J. Sed. Pet. 48 (1978) 519–538.

[17] A. Baker, P.L. Smart, W.L. Barnes, R.L. Edwards, A.R. Farrant, The Hekla 3 volcanic eruption recoded in a Scottish speleothem?, Holocene 5 (1995) 336–342.

[18] J.W. Valley, C.M. Graham, Ion microprobe analysis of oxygen isotope ratios in granulite facies magnetites – diffusive exchange as a guide to cooling history, Contrib. Mineral. Petrol. 109 (1991) 38–52.

[19] J. Veizer, R.W. Hinton, R.N. Clayton, A. Lerman, Chemical diagenesis of carbonates in thin-sections: ion microprobe as a trace element tool, Chem. Geol. 64 (1987) 225–237.

[20] P.K. Swart, Calibration of the ion microprobe for the quantitative determination of strontium, iron, manganese and magnesium in carbonate minerals, Anal. Chem. 62 (1990) 722–728.

[21] A. Mucci, J.W. Morse, Chemistry of low-temperature abiotic calcites: experimental studies on coprecipitation, stability, and fractionation, Rev. Aq. Sci. 3 (1990) 217–254.

[22] T. Oomori, H. Kaneshima, Y. Maezato, Y. Kitano, Distribution coefficient of Mg^{2+} ions between calcite and solution at 10–50°C, Mar. Chem. 20 (1987) 327–336.

[23] A. Mucci, Influence of temperature on the composition of magnesian calcite overgrowths precipitated from seawater, Geochim. Cosmochim. Acta 51 (1987) 1977–1984.

[24] E.A. Burton, L.M. Walter, The effects of PCO_2 and temperature on magnesium incorporation in calcite on seawater and $MgCl_2$–$CaCl_2$ solutions, Geochim. Cosmochim. Acta 55 (1991) 777–785.

[25] L.M. Henderson, F.C. Kracek, The fractional precipitation of barium and radium chromates, J. Am. Chem. Soc. 49 (1927) 739.

[26] T.C. Atkinson, T.J. Lawson, N.J. Hebdon, Karst Geomorphology, in: T.J. Lawson (Ed.), The Quaternary of Assynt and Coigach, Quat. Res. Assoc., Cambridge, 1995, pp. 61–86.

[27] T.M.L. Wigley, M.C. Brown, The physics of caves, in: T.D. Ford, C.H.D. Cullingford (Eds.), The Science of Speleology, Academic Press, London, 1976, pp. 329–358.

[28] S.T. Trudgill, I.M.S. Laidlaw, P.L. Smart, Soil water residence times and solute uptake on a dolomite bedrock–preliminary results, Earth Surf. Proc. 5 (1980) 91–100.

[29] M.R. Howson, A.D. Pethybridge, W.A. House, Synthesis and distribution coefficient of low magnesium calcites, Chem. Geol. 64 (1987) 79–87.

[30] J.L. Banner, Application of the trace element and isotope geochemistry of strontium to studies of carbonate diagenesis, Sedimentol. 42 (1995) 805–824.

[31] R.B. Lorens, Sr, Cd, Mn and Co distribution coefficients in calcite as a function of precipitation rate, Geochim. Cosmochim. Acta 45 (1981) 553–561.

[32] A.J. Tesoriero, J.F. Pankow, Solid solution partitioning of Sr^{2+}, Ba^{2+} and Cd^{2+} to calcite, Geochim. Cosmochim. Acta 60 (1996) 1053–1060.

[33] W. Dreybrodt, Processes in Karst Systems, Springer, Berlin, 1988.

[34] B. Huntley, I.C. Prentice, July temperatures in Europe from pollen data, 6000 years before present, Science 241 (1988) 687–690.

[35] L.B. Railsbeck, G.A. Brook, J. Chen, R. Kalin, C.J. Fleisher, Environmental controls on the petrology of a late Holocene speleothem from Botswana with annual layers of aragonite and calcite, J. Sed. Res. A64 (1994) 147–155.

[36] L.N. Plummer, Defining reactions and mass transfer in part of the Floridan aquifer, Water Res. Res. 13 (1977) 801–812.

[37] K.C. Lohmann, Geochemical patterns of meteoric diagenetic systems and their application to paleokarst, in: N.P. James, P.W. Choquette (Eds.), Paleokarst, Springer, New York, 1988, pp. 58–80.

[38] D. Langmuir, The geochemistry of some carbonate ground waters in central Pennsylvania, Geochim. Cosmochim. Acta 35 (1971) 1023–1045.

[39] D.W. Cowell, D.C. Ford, Hydrochemistry of a dolomite karst: the Bruce Peninsula of Ontario, Can. J. Earth Sci. 17 (1980) 520–526.

[40] C.A.J. Appelo, H.E. Beekman, A.W.A. Oosterbaan, Hydrochemistry of springs from dolomite reefs in the southern Alps of northern Italy, in: E. Eriksson (ed.), Hydrochemical balances of freshwater systems, IAHS Publ. 150 (1984) 125–138.

[41] I.J. Fairchild, A.F. Tooth, Y. Huang, A. Borsato, S. Frisia, F. McDermott, Spatial and temporal variations in water and stalactite chemistry in currently active caves: a precursor to interpretations of past climate, in: S. Bottrell (Ed.), Proc. Fourth Int. Symp. Geochem. Earth Surface, Ilkley, 1996.

[42] H.W. Rauch, W.B. White, Dissolution kinetics of carbonate rocks 1. Effects of lithology on dissolution rate, Water Res. Res. 13 (1977) 381–394.

[43] L. Chou, R.M. Garrels, R. Wollast, Comparative study of the kinetics and mechanisms of dissolution of carbonate minerals, Chem. Geol. 78 (1989) 269–282.

[44] M.E. Tucker, V.P. Wright, Carbonate Sedimentology, Blackwell, Oxford, 1990.

[45] D.A. Budd, Cenozoic dolomites of carbonate islands: their attributes and origin, Earth Sci. Rev. 42 (1997) 1–47.